Chapter 5

Finite element spaces

Finite element spaces are sets of continuous functions characterized by the finite element mesh Δ; a polynomial space defined on standard elements and the functions used for mapping the standard elements onto the elements of the mesh. We have seen a simple example of this in Section 2.5.3 where finite element spaces in one dimension were described. There the standard element was the interval $I = (-1, +1)$, the standard space, denoted by $\mathcal{S}^p$, was a polynomial space of degree p, and the mapping function was the linear function given by eq. (2.56). Finite element spaces in two dimensions are denoted by

$$\begin{aligned} S =& S(\Omega, \Delta, \mathbf{p}, \mathbf{Q}) := \\ & \{u \,|\, u \in E(\Omega),\ u(Q_x^{(k)}(\xi,\eta), Q_y^{(k)}(\xi,\eta)) \in \mathcal{S}^{p_k}(\Omega_{\mathrm{st}}),\ k = 1, 2, \ldots, M(\Delta)\} \end{aligned} \tag{5.1}$$

where $\mathbf{p}$ and $\mathbf{Q}$ represent, respectively, the arrays of the assigned polynomial degrees and the mapping functions. The expression

$$u(Q_x^{(k)}(\xi,\eta), Q_y^{(k)}(\xi,\eta)) \in \mathcal{S}^{p_k}(\Omega_{\mathrm{st}})$$

indicates that the basis functions defined on element Ω_k are mapped from the shape functions of a polynomial space defined on standard triangular and quadrilateral elements.

In this chapter the standard elements, the corresponding shape functions (i.e., standard basis function) and mapping functions are described for two and three-dimensional problems.

5.1 Standard elements in two dimensions

Two-dimensional finite element meshes are comprised of triangular and quadrilateral elements. The standard quadrilateral element will be denoted by $\Omega_{st}^{(q)}$ and the standard triangular element by $\Omega_{st}^{(t)}$. The definition of standard elements is arbitrary, however certain conveniences in mapping and assembly are

achieved when the standard elements are defined as shown in Fig. 5.1. Note that the sides of the elements have the same length (2) as in one-dimension.

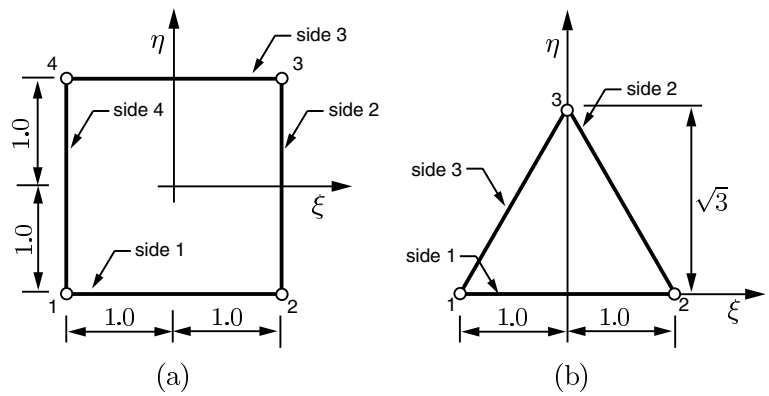

Figure 5.1: Standard quadrilateral and triangular elements $\Omega_{st}^{(q)}$ and $\Omega_{st}^{(t)}$.

5.2 Standard polynomial spaces

The standard polynomial spaces in two and three dimensions are generalizations of the standard polynomial space $\mathcal{S}^p(I_{\rm st})$ defined in Section 2.5.2. Whereas the polynomial degree could be characterized by a single number (p) in one dimension, in higher dimensions more than one interpretation is possible.

5.2.1 Trunk spaces

Trunk spaces, also called "serendipity" spaces, are polynomial spaces spanned by the set of monomials $\xi^i\eta^j$, $i,j = 0,1,2,\ldots,p$ subject to the restriction $i+j = 0,1,2,\ldots,p$. In the case of quadrilateral elements these are supplemented by one or two monomials of degree $p+1$:

1. Triangles: The dimension of the space is $n(p) = (p+1)(p+2)/2$. For example, the space $\mathcal{S}^6(\Omega_{st}^{(t)})$ is spanned by the 28 monomial terms indicated in Fig. 5.2. In other words, $\mathcal{S}^p(\Omega_{st}^{(t)})$ spans all polynomials of degree p.

2. Quadrilaterals: Monomials of degree less than or equal to p are supplemented by $\xi\eta$ for $p = 1$ and by $\xi^p\eta$, $\xi\eta^p$ for $p \geq 2$. For example, the space $\mathcal{S}^4(\Omega_{st}^{(q)})$ is spanned by the 17 monomial terms indicated in Fig. 5.2. The dimension of space $\mathcal{S}^p(\Omega_{st}^{(q)})$ is

$$n(p) = \begin{cases} 4p & \text{for } p \leq 3 \\ 4p + (p-2)(p-3)/2 & \text{for } p \geq 4 \end{cases} \tag{5.2}$$

which spans all polynomials of degree p.

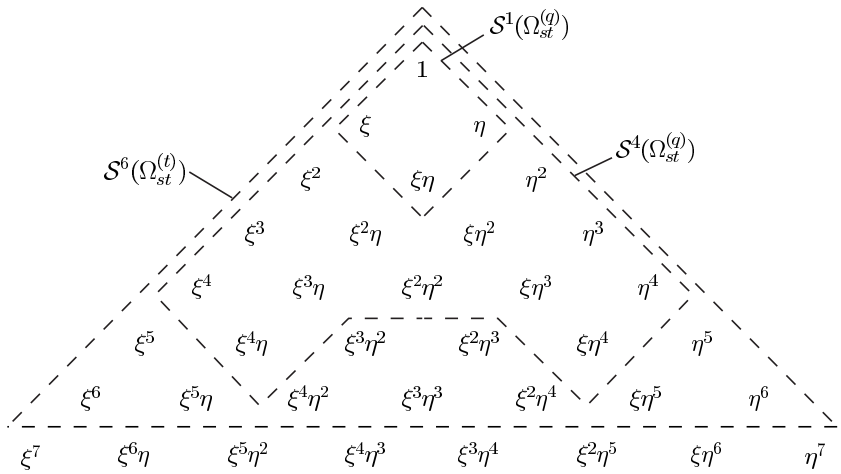

Figure 5.2: Trunk space. Illustration of spanning sets for $\mathcal{S}^1(\Omega_{st}^{(q)})$, $\mathcal{S}^4(\Omega_{st}^{(q)})$ and $\mathcal{S}^6(\Omega_{st}^{(t)})$.

5.2.2 Product spaces

In two dimensions product spaces are spanned by the monomials $1,\ \xi,\ \xi^2,\ \ldots,\ \xi^p$, $1,\ \eta,\ \eta^2,\ \ldots,\ \eta^q$ and their products. Thus the dimension of product spaces is $n(p,q) = (p+1)(q+1)$. Product spaces on triangles will be denoted by $\mathcal{S}^{p,q}(\Omega_{st}^{(t)})$ and on quadrilaterals by $\mathcal{S}^{p,q}(\Omega_{st}^{(q)})$. The spanning set of monomials for the space $\mathcal{S}^{4,2}(\Omega_{st}^{(q)})$ is illustrated in Fig. 5.3.

5.3 Shape functions

As in the one-dimensional case, we will discuss two types of shape functions: Shape functions based on Lagrange polynomials and hierarchic shape functions based on the integrals of Legendre polynomials. We will use the notation $N_i(\xi,\eta)$ $(i = 1, 2, \ldots, n)$ for both. The shape functions in two dimensions along the sides of each element are the same as the shape functions defined for the one-dimensional standard element I_{st}.

5.3.1 Lagrange shape functions

Elements with shape functions that span $\mathcal{S}^p(\Omega_{st}^{(t)})$ and $\mathcal{S}^p(\Omega_{st}^{(q)})$ with $p = 1$ and $p = 2$ are widely used in engineering practice. Each of the Lagrange shape functions are unity in one of the node points and zero in the other node points. Therefore the approximating function u can be written as

$$u(\xi,\eta) = \sum_{i=1}^{n} u_i N_i(\xi,\eta)$$

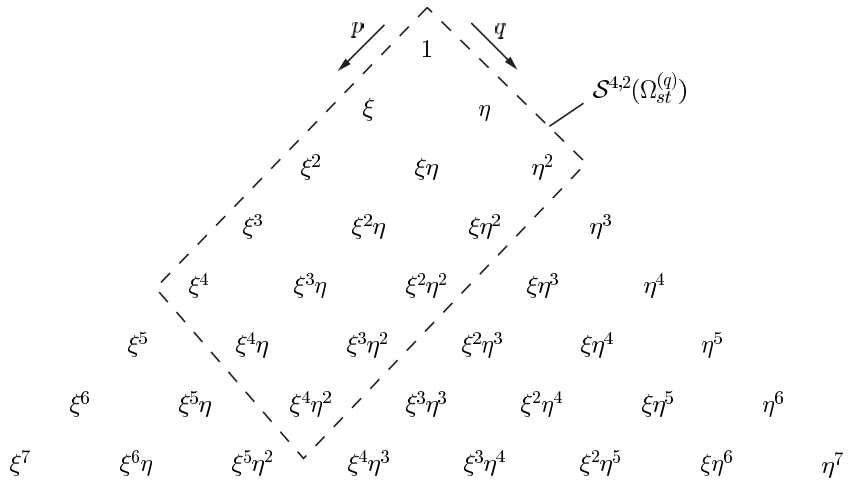

Figure 5.3: Product space. Illustration of spanning set for the space $\mathcal{S}^{4,2}(\Omega_{st}^{(q)})$.

where u_i is the value of u in the ith node point.

Quadrilateral elements

The shape functions of four-node quadrilateral elements span the space $\mathcal{S}^1(\Omega_{st}^{(q)})$:

$$N_1(\xi,\eta) := \frac{1}{4}(1-\xi)(1-\eta) \tag{5.3}$$

$$N_2(\xi,\eta) := \frac{1}{4}(1+\xi)(1-\eta) \tag{5.4}$$

$$N_3(\xi,\eta) := \frac{1}{4}(1+\xi)(1+\eta) \tag{5.5}$$

$$N_4(\xi,\eta) := \frac{1}{4}(1-\xi)(1+\eta) \tag{5.6}$$

The shape functions of eight-node quadrilateral elements span the space $\mathcal{S}^2(\Omega_{st}^{(q)})$. The shape functions corresponding to the vertex nodes are:

$$N_1(\xi,\eta) := \frac{1}{4}(1-\xi)(1-\eta)(-\xi-\eta-1) \tag{5.7}$$

$$N_2(\xi,\eta) := \frac{1}{4}(1+\xi)(1-\eta)(\xi-\eta-1) \tag{5.8}$$

$$N_3(\xi,\eta) := \frac{1}{4}(1+\xi)(1+\eta)(\xi+\eta-1) \tag{5.9}$$

$$N_4(\xi,\eta) := \frac{1}{4}(1-\xi)(1+\eta)(-\xi+\eta-1) \tag{5.10}$$

and the shape functions corresponding to the mid-side nodes are:

$$N_5(\xi,\eta) := \frac{1}{2}(1-\xi^2)(1-\eta) \tag{5.11}$$

$$N_6(\xi,\eta) := \frac{1}{2}(1+\xi)(1-\eta^2) \tag{5.12}$$

$$N_7(\xi,\eta) := \frac{1}{2}(1-\xi^2)(1+\eta) \tag{5.13}$$

$$N_8(\xi,\eta) := \frac{1}{2}(1-\xi)(1-\eta^2). \tag{5.14}$$

Note that if we denote the coordinates of the vertices and the midpoints of the sides by (ξ_i, η_i), $i = 1, 2, \ldots, 8$, then $N_i(\xi_j, \eta_j) = \delta_{ij}$.

The shape functions of the nine-node quadrilateral element span $\mathcal{S}^{2,2}(\Omega_{st}^{(q)})$ (i.e., the product space). In addition to the four nodes located in the vertices and the four nodes located in the mid-points of the sides there is a node in the center of the element. Construction of these shape functions is left to the reader in the following exercise.

Exercise 5.3.1 Write down the shape functions for the nine-node quadrilateral element. Sketch the shape function associated with the node in the center of the element and one of the vertex shape functions and one of the side shape functions.

Triangular elements

The shape functions for triangular elements are usually written in terms of the triangular coordinates, defined as follows:

$$L_1 := \frac{1}{2}\left(1-\xi-\frac{\eta}{\sqrt{3}}\right) \tag{5.15}$$

$$L_2 := \frac{1}{2}\left(1+\xi-\frac{\eta}{\sqrt{3}}\right) \tag{5.16}$$

$$L_3 := \frac{\eta}{\sqrt{3}}\cdot \tag{5.17}$$

Note that L_i is unity at node i and zero on the side opposite to node i. Also, $L_1+L_2+L_3 = 1$. The space $\mathcal{S}^1(\Omega_{st}^{(t)})$ is spanned by the following shape functions:

$$N_i := L_i \quad i = 1, 2, 3. \tag{5.18}$$

These elements are called "three-node triangles". For the six-node triangles the shape functions are:

$$N_1 := L_1(2L_1 - 1) \tag{5.19}$$
$$N_2 := L_2(2L_2 - 1) \tag{5.20}$$
$$N_3 := L_3(2L_3 - 1) \tag{5.21}$$
$$N_4 := 4L_1L_2 \tag{5.22}$$
$$N_5 := 4L_2L_3 \tag{5.23}$$
$$N_6 := 4L_3L_1 \tag{5.24}$$

which span $\mathcal{S}^2(\Omega_{st}^{(t)})$.

5.3.2 Hierarchic shape functions

Hierarchic shape functions based on the integrals of Legendre polynomials are described for the nodes, sides and vertices of quadrilateral and triangular elements. The shape functions associated with nodes and sides are the same for the product and trunk spaces. Only the number of internal shape functions is different. .

Quadrilateral elements

The nodal shape functions are the same as those for the four-node quadrilateral, given by equations (5.3) to (5.6).

The side shape functions are constructed by multiplying the shape functions $N_3,\ N_4,\ \ldots,$ defined for the one-dimensional element (see Fig. 2.8), by linear blending functions. We define:

$$\phi_k(s) := \sqrt{\frac{2k-1}{2}} \int_{-1}^{s} P_{k-1}(t)\, dt \quad k = 2, 3, \ldots \tag{5.25}$$

Note that the index k represents the polynomial degree. The shape functions of degree $p \geq 2$ are defined for the four sides as follows:

$$\text{side 1:} \qquad N_k^{(1)}(\xi, \eta) := \frac{1}{2}(1 - \eta)\phi_k(\xi) \tag{5.26}$$
$$\text{side 2:} \qquad N_k^{(2)}(\xi, \eta) := \frac{1}{2}(1 + \xi)\phi_k(\eta) \tag{5.27}$$
$$\text{side 3:} \qquad N_k^{(3)}(\xi, \eta) := \frac{1}{2}(1 + \eta)\phi_k(-\xi) \tag{5.28}$$
$$\text{side 4:} \qquad N_k^{(4)}(\xi, \eta) := \frac{1}{2}(1 - \xi)\phi_k(-\eta) \tag{5.29}$$

where $k = 2, 3, \ldots, p$. Thus there are $4(p-1)$ side shape functions. The argument of ϕ_k is negative for sides 3 and 4 because the positive orientation of the sides is counterclockwise. This will affect shape functions of odd degrees only.

The internal shape functions are zero on the sides. For the trunk space there are $(p-2)(p-3)/2$ internal shape functions ($p \geq 4$) constructed from the products of ϕ_k:

$$N_p^{(k,l)}(\xi,\eta) := \phi_k(\xi)\phi_l(\eta) \qquad k,l = 2,3,\ldots,p, \quad k+l = 4,5,\ldots,p. \tag{5.30}$$

The shape functions are assigned unique sequential numbers, as shown for in Fig. 5.4. For the product space there are $(p-1)(q-1)$ internal shape functions, defined for $p,q \geq 2$ by

$$N_{pq}^{(k,l)}(\xi,\eta) := \phi_k(\xi)\phi_l(\eta), \quad k = 2,3,\ldots,p,\ l = 2,3,\ldots,q,\ k+l \leq p+q. \tag{5.31}$$

Triangular elements

The nodal shape functions are the same as those for the three-node triangles, given by eq. (5.18). The side shape functions are constructed as follows: Define:

$$\tilde{\phi}_k(s) := 4\frac{\phi_k(s)}{1-s^2} \quad k = 2,3,\ldots \tag{5.32}$$

where $\phi_k(s)$ is the function defined by eq. (5.25). For example,

$$\tilde{\phi}_2(s) = -\sqrt{6}, \quad \tilde{\phi}_3(s) = -\sqrt{10}s, \quad \tilde{\phi}_4(s) = -\sqrt{\frac{7}{8}}(5s^2-1), \text{ etc.}$$

Using

$$s = \begin{cases} L_2 - L_1 & \text{for side 1} \\ L_3 - L_2 & \text{for side 2} \\ L_1 - L_3 & \text{for side 3} \end{cases} \tag{5.33}$$

the definition of the side shape functions is

$$\text{side 1:} \qquad N_k^{(1)}(L_1,L_2,L_3) := L_1L_2\tilde{\phi}_k(L_2-L_1) \tag{5.34}$$

$$\text{side 2:} \qquad N_k^{(2)}(L_1,L_2,L_3) := L_2L_3\tilde{\phi}_k(L_3-L_2) \tag{5.35}$$

$$\text{side 3:} \qquad N_k^{(3)}(L_1,L_2,L_3) := L_3L_1\tilde{\phi}_k(L_1-L_3) \tag{5.36}$$

where $k = 2,3,\ldots,p$. Thus there are $3(p-1)$ side shape functions.

For the trunk space there are $(p-1)(p-2)/2$ internal shape functions ($p \geq 3$) defined as follows:

$$N_p^{(k,l)} := L_1L_2L_3P_k(L_2-L_1)P_l(2L_3-1) \quad k,l = 0,1,2,\ldots,p-3 \tag{5.37}$$

where $k+l \leq p-3$ and P_k is the kth Legendre polynomial.

Exercise 5.3.2 Sketch the shape function $N_3^{(2)}(L_1,L_2,L_3)$.

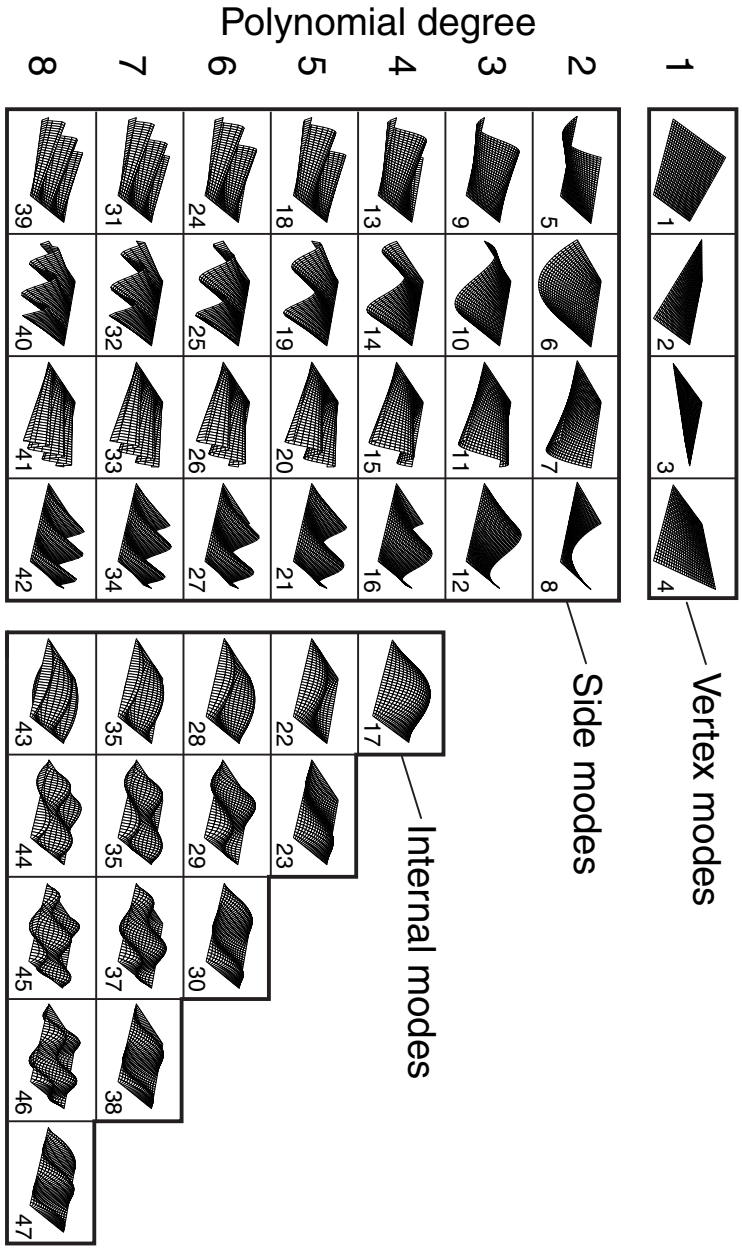

Figure 5.4: Hierarchic shape functions for quadrilateral elements. Trunk space, $p = 1$ to $p = 8$.

5.4 Mapping functions in two dimensions

Mapping functions are used for two purposes: (a) To map the standard element to the corresponding elements of the mesh and (b) to impart certain properties to the mapped polynomials so that they will be better suited for approximating some known local characteristics of the exact solution. The following discussion is concerned with the first objective only.

5.4.1 Isoparametric mapping

Isoparametric mapping utilizes the Lagrange shape functions described in Section 5.3.1. The most commonly used isoparametric mapping procedures are the linear and quadratic mappings.

Quadrilateral elements

Linear mapping of quadrilateral elements from the standard quadrilateral element shown in Fig. 5.1(a) to the kth element is defined by

$$x = Q_x^{(k)}(\xi, \eta) := \sum_{i=1}^{4} N_i(\xi, \eta) X_i \tag{5.38}$$

$$y = Q_y^{(k)}(\xi, \eta) := \sum_{i=1}^{4} N_i(\xi, \eta) Y_i \tag{5.39}$$

where (X_i, Y_i) are the coordinates of vertex i of the kth element numbered in counterclockwise order and N_i are the shape functions defined by equations (5.3) through (5.6).

Quadratic mapping of quadrilateral elements from the standard quadrilateral element is defined by:

$$x = Q_x^{(k)}(\xi, \eta) := \sum_{i=1}^{8} N_i(\xi, \eta) X_i \tag{5.40}$$

$$y = Q_y^{(k)}(\xi, \eta) := \sum_{i=1}^{8} N_i(\xi, \eta) Y_i \tag{5.41}$$

where (X_i, Y_i) are the coordinates of the four vertices numbered in counterclockwise order and the mid-points of the four sides also numbered in counterclockwise order. The side between nodes 1 and 2 is the first side. N_i are the shape functions defined by equations (5.7) through (5.14). Quadratic isoparametric mapping of a quadrilateral element and typical numbering of the node points are illustrated in Fig. 5.5(a).

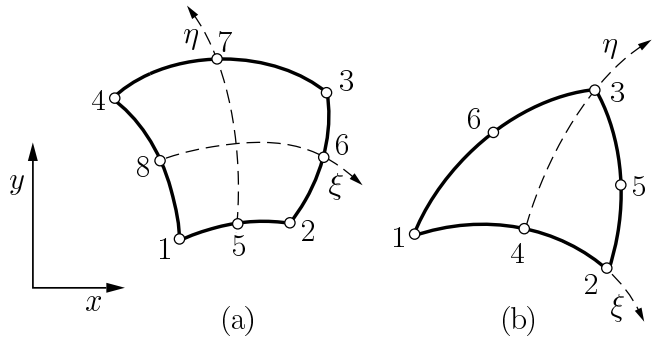

Figure 5.5: Isoparametric quadrilateral and triangular elements.

Triangular elements

Linear mapping of triangles from the standard triangular element shown in Fig. 5.1(b) to the kth element is defined by

$$x = Q_x^{(k)}(L_1, L_2, L_3) := \sum_{i=1}^{3} L_i X_i \tag{5.42}$$

$$y = Q_y^{(k)}(L_1, L_2, L_3) := \sum_{i=1}^{3} L_i Y_i. \tag{5.43}$$

Quadratic isoparametric mapping of triangular elements from the standard quadrilateral element is given by

$$x = Q_x^{(k)}(L_1, L_2, L_3) := \sum_{i=1}^{6} N_i(L_1, L_2, L_3) X_i \tag{5.44}$$

$$y = Q_y^{(k)}(L_1, L_2, L_3) := \sum_{i=1}^{6} N_i(L_1, L_2, L_3) Y_i \tag{5.45}$$

where N_i are the shape functions defined by equations (5.19) through (5.24). The mapping of a triangular element and typical numbering of the node points are illustrated in Fig. 5.5(b).

The term "isoparametric mapping" is meant to convey the idea that the same shape functions are used for providing topological descriptions for elements as for the element-level approximations. If the mapping is of lower (resp. higher) polynomial degree than the approximating functions then it is said to be subparametric (resp. superparametric).

Remark 5.4.1 The mapped shape functions are polynomials only in the special cases when the standard triangle is mapped into a straight-side triangle and when the standard quadrilateral element is mapped into a parallelogram. In general the mapped shape functions are not polynomials. Mapped shape

functions are called 'pull-back polynomials'. The accuracy of finite element approximation is governed by the properties of the pull-back polynomials. Depending on exact solution, approximation by the pull-back polynomials can be better or worse than approximation by polynomials. In some cases the mapping is designed to improve the approximation.

Exercise 5.4.1 Show that quadratic parametric mapping applied to straight-side triangular and quadrilateral elements is identical to linear mapping.

5.4.2 Mapping by the blending function method.

To illustrate the method, let us consider a simple case where only one side (side 2) of a quadrilateral element is curved, as shown in Figure 5.6. The curve $x = x_2(\eta)$, $y = y_2(\eta)$ is given in parametric form with $-1 \leq \eta \leq 1$. We can now write:

$$\begin{aligned} x =& \frac{1}{4}(1-\xi)(1-\eta)X_1 + \frac{1}{4}(1+\xi)(1-\eta)X_2 + \frac{1}{4}(1+\xi)(1+\eta)X_3 \\ &+\frac{1}{4}(1-\xi)(1+\eta)X_4 + \left(x_2(\eta) - \frac{1-\eta}{2}X_2 - \frac{1+\eta}{2}X_3\right)\frac{1+\xi}{2} \end{aligned} \tag{5.46}$$

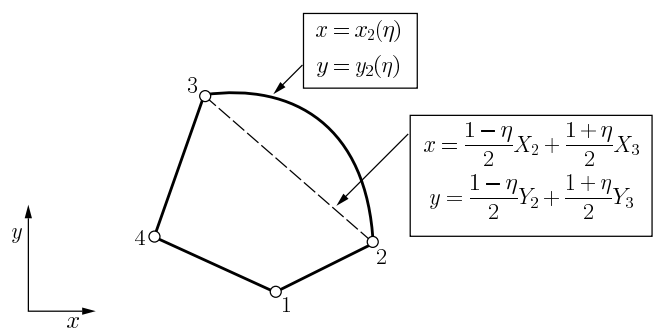

Figure 5.6: Quadrilateral element with one curved side.

Observe that the first four terms in this expression are the linear mapping terms given by eq. (5.38). The fifth term is the product of two functions: One function, the bracketed expression, represents the difference between $x_2(\eta)$ and the x - coordinates of the chord that connects points $(X_2,\ Y_2)$ and $(X_3,\ Y_3)$. The other function is the linear blending function $(1+\xi)/2$ which is unity along side 2 and zero along side 4. Therefore we can write:

$$x = \frac{1}{4}(1-\xi)(1-\eta)X_1 + \frac{1}{4}(1-\xi)(1+\eta)X_4 + x_2(\eta)\frac{1+\xi}{2}. \tag{5.47}$$

Similarly:

$$y = \frac{1}{4}(1-\xi)(1-\eta)Y_1 + \frac{1}{4}(1-\xi)(1+\eta)Y_4 + y_2(\eta)\frac{1+\xi}{2}. \tag{5.48}$$

In the general case all sides may be curved. We write the curved sides in parametric form:

$$x = x_i(s), \quad y = y_i(s), \quad -1 \le s \le +1 \quad \text{where } s = \begin{cases} \xi & \text{on sides 1 and 3} \\ \eta & \text{on sides 2 and 4} \end{cases}$$

and the subscripts represent the side numbers of the standard element. In this case the mapping functions are:

$$\begin{aligned} x =& \frac{1}{2}(1-\eta)x_1(\xi) + \frac{1}{2}(1+\xi)x_2(\eta) + \frac{1}{2}(1+\eta)x_3(\xi) + \frac{1}{2}(1-\xi)x_4(\eta) \\ &-\frac{1}{4}(1-\xi)(1-\eta)X_1 - \frac{1}{4}(1+\xi)(1-\eta)X_2 - \frac{1}{4}(1+\xi)(1+\eta)X_3 \\ &-\frac{1}{4}(1-\xi)(1+\eta)X_4 \end{aligned} \tag{5.49}$$

$$\begin{aligned} y =& \frac{1}{2}(1-\eta)y_1(\xi) + \frac{1}{2}(1+\xi)y_2(\eta) + \frac{1}{2}(1+\eta)y_3(\xi) + \frac{1}{2}(1-\xi)y_4(\eta) \\ &-\frac{1}{4}(1-\xi)(1-\eta)Y_1 - \frac{1}{4}(1+\xi)(1-\eta)Y_2 - \frac{1}{4}(1+\xi)(1+\eta)Y_3 \\ &-\frac{1}{4}(1-\xi)(1+\eta)Y_4. \end{aligned} \tag{5.50}$$

The inverse mapping, that is: $\xi = Q_\xi^{(k)}(x,y)$, $\eta = Q_\eta^{(k)}(x,y)$, cannot be given explicitly in general, but (ξ, η) can be computed very efficiently for any given (x, y) by means of the Newton-Raphson method or a similar procedure.

Exercise 5.4.2 Refer to Fig. 5.7(a). Show that the mapping of the quadrilateral element by the blending function method is:

$$\begin{aligned} x =& r_i \cos(\theta_m + \eta\theta_d)\frac{1-\xi}{2} + r_o \cos(\theta_m + \eta\theta_d)\frac{1+\xi}{2} \\ y =& r_i \sin(\theta_m + \eta\theta_d)\frac{1-\xi}{2} + r_o \sin(\theta_m + \eta\theta_d)\frac{1+\xi}{2} \end{aligned}$$

where

$$\theta_m := \frac{\theta_1 + \theta_2}{2}, \quad \theta_d := \frac{\theta_2 - \theta_1}{2}.$$

Exercise 5.4.3 Refer to Fig. 5.7(b). A quadrilateral element is bounded by two circles. The centers of the circles are offset as shown. Write down the mapping by the blending function method in terms of the given parameters. Hint: Using the law of cosines, the radius of the arc between node 2 and node 3 is:

$$r_{2-3} = -e\sin\theta + \sqrt{r_o^2 - e^2\cos^2\theta}$$

where θ is the angle measured from the x-axis.

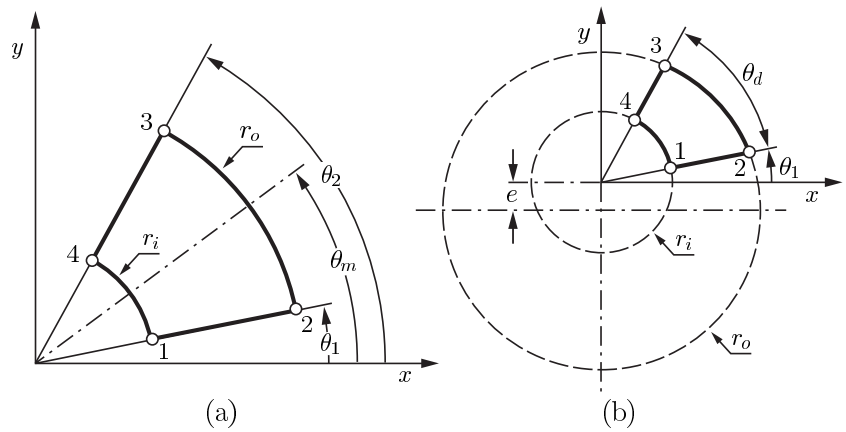

Figure 5.7: Quadrilateral elements bounded by circular segments.

5.4.3 Mapping of high order elements

High order elements are usually mapped by the blending function method with the bounding curves approximated by polynomial functions, similar to isoparametric mapping. The reasons for this are that (a) the boundary curves are generally not available in analytical form and (b) standard treatment of all bounding curves is preferable from the point of view of implementation. For example, the boundaries of a domain are typically represented by a collection of splines in computer aided design (CAD) software products. In the interest of generality of implementation, the bounding curves are interpolated using the Lagrangian basis functions defined in eq. (2.60). The quality of the approximation depends on the choice of the interpolation points. Specifically, the interpolation points must be such that, for the given polynomial degree of interpolation, the interpolation function is close to the best possible approximation of the boundary curve by polynomials in maximum norm. The abscissas of the Lobatto points[1] are close to the optimal interpolation points. For details we refer to [14].

5.4.4 Rigid body rotations

In two-dimensional elasticity infinitesimal rigid body rotation is represented by the displacement vector $\vec{u} = C\{y \;\; -x\}^T$. Having introduced the mappings $x = Q_x^{(k)}(\xi,\eta)$, $y = Q_y^{(k)}(\xi,\eta)$, infinitesimal rigid body rotations are represented exactly by element k only when $Q_x^{(k)}(\xi,\eta) \in \mathcal{S}^{p_k}(\Omega_{\rm st})$ and $Q_y^{(k)}(\xi,\eta) \in \mathcal{S}^{p_k}(\Omega_{\rm st})$. Iso- and subparametric mappings satisfy this condition, hence rigid body rotation imposed on an element will not induce strains. Superparametric mappings and mapping by the blending function method when the sides are not polynomials, or are polynomials of degree higher than p_k, do not satisfy this condition.

[1] See Appendix B.

It has been argued that for this reason only iso- and subparametric mappings should be employed.

This argument is flawed, however. One should view this question in the following light: Errors are introduced when rigid body rotations are not represented exactly and also by errors in the approximation of boundary curves. With the blending function method analytic curves, such as circles, are represented exactly, but the rigid body rotation terms are approximated. With iso- and subparametric mappings the boundaries are approximated but the rigid body rotation terms are represented exactly. In either case the errors of approximation will go to zero as the number of degrees of freedom is increased whether by mesh refinement or increasing the polynomial degrees. This is illustrated by the following exercises.

Exercise 5.4.4 Refer to Fig. 5.7(a). Let $\theta_1 = 0$, $\theta_2 = 60°$, $r_i = 1.0$ and $r_o = 2.0$. Use $E = 200$ GPa, $\nu = 0.3$, plane strain. Impose nodal displacements consistent with rigid body rotation about the origin: $\mathbf{u} = C\{y\ -x\}$. For example let $u_x^{(1)} = 0$, $u_y^{(1)} = Cr_i$, $u_y^{(2)} = Cr_o$ where the superscripts indicate the node numbers and C is the angle of rotation (in radians) about the positive z axis. Let $C = 0.1$ and compute the maximum equivalent strain[2] for $p = 1, 2, \ldots, 6$. Very rapid convergence to zero will be seen[3].

Exercise 5.4.5 Repeat Exercise 5.4.4 using uniform mesh refinement and p fixed at $p = 1$ and $p = 2$. Plot the maximum equivalent strain vs. the number of degrees of freedom.

Remark 5.4.2 The constant function is in the finite element space $\mathcal{S}^{p_k}(\Omega_{\rm st})$ independently of the mapping. Therefore rigid body displacements are represented exactly.

5.5 Elements in three dimensions

Three-dimensional finite element meshes are comprised of hexahedral, tetrahedral, pentahedral elements, less frequently other types of elements, such as pyramid elements, are used. The standard hexahedral element, denoted by $\Omega_{st}^{(h)}$, is the set of points $-1 \le \xi, \eta, \zeta \le +1$. The standard tetrahedral element, denoted by $\Omega_{st}^{(th)}$ and the standard pentahedral element, denoted by $\Omega_{st}^{(p)}$, are shown in Fig. 5.8. Note that the edges of the elements have the length 2.0, as in one and two dimensions.

The shape functions are analogous to those in one and two dimensions. For example, the eight-node hexahedral element has vertex shape functions such as:

$$N_1 = \frac{1}{8}(1-\xi)(1-\eta)(1-\zeta).$$

[2]The equivalent strain is proportional to the root-mean-square of the differences of principal strains and therefore it is an indicator of the maximum shearing strain.

[3]Curves are approximated by polynomials of degree 5 in StressCheck. This is a default value that can be changed by setting a parameter. When the default value is used then the mapping is superparametric for $p \le 4$, isoparametric at $p = 5$ and subparametric for $p \ge 6$.

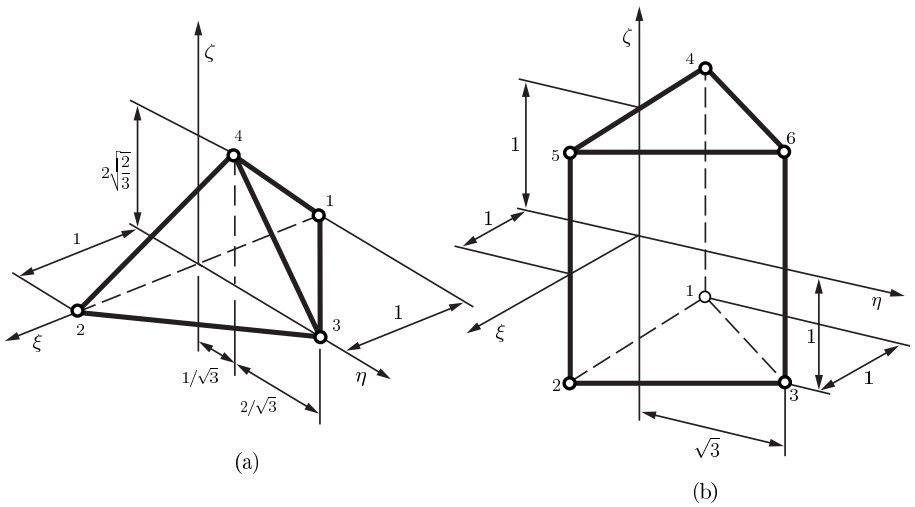

Figure 5.8: The standard tetrahedral and pentahedral elements $\Omega_{st}^{(th)}$ and $\Omega_{st}^{(p)}$.

The 20-node hexahedron is a generalization of the 8-node quadrilateral element to three dimensions. Similarly, the 4-node and 10-node tetrahedra are generalizations of the 3-node and 6-node triangles.

The hierarchic shape functions are also analogous to the shape functions defined in one and two dimensions. A detailed description of shape functions for hexahedral elements can be found in [20]. The shape functions associated with the edges and faces are the same along the edges and on the faces as in two dimensions. For example, the edge shape function of the pentahedral element, associated with the edge between nodes 1 and 2, corresponding to $p = 2$ is:

$$N_7 = L_1 L_2 \tilde{\phi}_2 (L_2 - L_1) \frac{1-\zeta}{2}$$

where $\tilde{\phi}_2$ is defined by eq. (5.32). The face shape function of the pentahedral element, associated with the face defined by nodes 1, 2 and 3, at $p = 3$ is:

$$N_{13} = L_1 L_2 L_3 \frac{1-\zeta}{2}.$$

The internal shape functions of the pentahedral elements are the products of the internal shape functions defined for the triangular elements in eq. (5.37) and the function $\phi_k(\eta)$ defined by eq. (5.25).

5.6 Integration and differentiation

In Section 2.5.4, the coefficients of the stiffness matrix, Gram matrix and the right-hand side vector were computed on the standard element. In two and

three dimensions the corresponding procedures are analogous, however, with the exception of some important special cases, the mappings are generally nonlinear.

The mapping functions

$$x = Q_x^{(k)}(\xi, \eta, \zeta), \quad y = Q_y^{(k)}(\xi, \eta, \zeta), \quad z = Q_z^{(k)}(\xi, \eta, \zeta) \tag{5.51}$$

map a standard element Ω_{st} onto the kth element Ω_k. In the following we will drop the superscript when it is clear that we refer to the mapping of the kth element. A mapping is said to be proper when the following three conditions are met: (a) The mapping functions Q_x, Q_y, Q_z are single valued functions of ξ, η, ζ and possess continuous first derivatives; (b) the Jacobian determinant $|J|$ (defined below) does not vanish anywhere in Ω_{st}, and (c) $|J|$ is positive in every point of Ω_{st}. The mapping functions used in FEA must meet these criteria.

5.6.1 Volume and area integrals

Volume integrals on the kth element are computed on the corresponding standard element. The volume integral of a scalar function $F(x, y, z)$ on Ω_k is:

$$\int_{\Omega_k} F(x, y, z)\, dxdydz = \int_{\Omega_{\text{st}}} \mathcal{F}(\xi, \eta, \zeta)|J|\, d\xi d\eta d\zeta \tag{5.52}$$

where $\mathcal{F}(\xi, \eta, \zeta) := F(Q_x(\xi,\ \eta, \zeta),\ Q_y(\xi, \eta, \zeta), Q_z(\xi, \eta, \zeta))$, $|J|$ is the determinant of the Jacobian matrix[4], called the Jacobian determinant. The Jacobian determinant in eq. (5.52) arises from the definition of the differential volume: Let us denote the position vector of an arbitrary point P in the element $\bar{\Omega}_k$ by $\vec{r}$:

$$\vec{r} := x\vec{e}_x + y\vec{e}_y + z\vec{e}_z \tag{5.53}$$

where $\vec{e}_x$, $\vec{e}_y$, $\vec{e}_z$ are the orthogonal basis vectors of a right-handed Cartesian coordinate system. By definition, the differential volume is understood to be the scalar triple product:

$$dV := \left(\frac{\partial \vec{r}}{\partial x}dx \times \frac{\partial \vec{r}}{\partial y}dy\right) \cdot \frac{\partial \vec{r}}{\partial z}dz = (\vec{e}_x \times \vec{e}_y) \cdot \vec{e}_z\, dxdydz = dxdydz.$$

Given the change of variables of eq. (5.51), the analogous expression is:

$$dV = \left(\frac{\partial \vec{r}}{\partial \xi}d\xi \times \frac{\partial \vec{r}}{\partial \eta}d\eta\right) \cdot \frac{\partial \vec{r}}{\partial \zeta}d\zeta = \begin{vmatrix} \dfrac{\partial x}{\partial \xi} & \dfrac{\partial y}{\partial \xi} & \dfrac{\partial z}{\partial \xi} \\ \dfrac{\partial x}{\partial \eta} & \dfrac{\partial y}{\partial \eta} & \dfrac{\partial z}{\partial \eta} \\ \dfrac{\partial x}{\partial \zeta} & \dfrac{\partial y}{\partial \zeta} & \dfrac{\partial z}{\partial \zeta} \end{vmatrix} d\xi d\eta d\zeta \equiv |J|\, d\xi d\eta d\zeta \tag{5.54}$$

[4]Carl Gustav Jacob Jacobi 1804-1851.

which was to be shown. The vectors $\partial\vec{r}/\partial\xi$, $\partial\vec{r}/\partial\eta$, $\partial\vec{r}/\partial\zeta$ are a set of right-handed basis vectors, that is, their scalar triple product yields a positive number. If the Jacobian determinant is negative then the right-handed coordinate system is transformed into a left-handed one in which case the mapping is improper.

In two dimensions the mapping is

$$x = Q_x(\xi,\eta), \quad y = Q_y(\xi,\eta), \quad z = Q_z(\zeta) = \frac{t_z}{2}\zeta$$

where t_z is the thickness, see Fig. 3.3. When the thickness is constant then the integration in the transverse (ζ) direction can be performed explicitly and only an area integral needs to be evaluated:

$$dV = t_z\, dA = t_z \begin{vmatrix} \dfrac{\partial x}{\partial \xi} & \dfrac{\partial y}{\partial \xi} \\ \dfrac{\partial x}{\partial \eta} & \dfrac{\partial y}{\partial \eta} \end{vmatrix} d\xi d\eta \tag{5.55}$$

In the finite element method the integrations are performed by numerical quadrature, details of which are given in Appendix B. The minimum number of quadrature points depends on the polynomial degree of the shape functions: When the mapping is linear and the material properties are constant then the coefficients of the stiffness matrix should be exact (up to numerical round-off errors) otherwise the stiffness matrix may become singular. When the material properties vary or the mapping is non-linear then the number of integration points should be increased so that the errors in the stiffness coefficients are small. Similar considerations apply to the load vector.

Exercise 5.6.1 Show that the Jacobian matrix of straight-side triangular elements, that is, triangular elements mapped by eq. (5.42) and eq. (5.43), is independent of L_1, L_2 and L_3 and show that the area of a triangle in terms of its vertex coordinates (X_i, Y_i), $i = 1, 2, 3$ is:

$$A = \frac{X_1(Y_2 - Y_3) + X_2(Y_3 - Y_1) + X_3(Y_1 - Y_2)}{2}.$$

Exercise 5.6.2 Show that for straight side quadrilaterals the Jacobian determinant is constant only if the quadrilateral element is a parallelogram.

5.6.2 Surface and contour integrals

Given the mapping functions, each face is parameterized by imposing the appropriate restriction on the mapping function. For example, if integration is to be performed on the face of a hexahedron that corresponds to $\zeta = 1$ then, referring to eq. (5.51), the parametric form of the surface becomes:

$$x = Q_x(\xi,\eta,1), \quad y = Q_y(\xi,\eta,1), \quad z = Q_z(\xi,\eta,1) \tag{5.56}$$

and, using the definition of $\vec{r}$ given in (5.53), the surface integral of a scalar function $F(x, y, z)$ is:

$$\int\int_{(\partial\Omega_k)_{\zeta=1}} F(x, y, z)\, dS = \int_{-1}^{+1}\int_{-1}^{+1} \mathcal{F}(\xi, \eta, 1) \left| \frac{\partial \vec{r}}{\partial \xi} \times \frac{\partial \vec{r}}{\partial \eta} \right| d\xi d\eta$$

where $\mathcal{F}$ is obtained from F by replacing x, y, z with the mapping functions Q_x, Q_y. Q_z. The treatment of the other faces is analogous.

In two dimensions the contour integral of a scalar function $F(x, y)$ on the side of a quadrilateral element corresponding to $\eta = 1$ is:

$$\int_{(\partial\Omega_k)_{\eta=1}} F(x, y)\, ds = \int_{-1}^{+1} \mathcal{F}(\xi, 1) \left| \frac{d\vec{r}}{d\xi} \right| d\xi.$$

The other sides are treated analogously. The positive sense of the contour integral is counterclockwise.

5.6.3 Differentiation

The inverse of the Jacobian matrix plays an important role in the computation of stiffness matrices and in post-processing operations. In particular, the approximating functions and hence the solution are known in terms of the shape functions defined on standard elements. Therefore differentiation with respect to x, y and z has to be expressed in terms of differentiation with respect to ξ, η, ζ. Using the chain rule we have:

$$\begin{Bmatrix} \dfrac{\partial}{\partial \xi} \\ \\ \dfrac{\partial}{\partial \eta} \\ \\ \dfrac{\partial}{\partial \zeta} \end{Bmatrix} = \begin{bmatrix} \dfrac{\partial x}{\partial \xi} & \dfrac{\partial y}{\partial \xi} & \dfrac{\partial z}{\partial \xi} \\ \\ \dfrac{\partial x}{\partial \eta} & \dfrac{\partial y}{\partial \eta} & \dfrac{\partial z}{\partial \eta} \\ \\ \dfrac{\partial x}{\partial \zeta} & \dfrac{\partial y}{\partial \zeta} & \dfrac{\partial z}{\partial \zeta} \end{bmatrix} \begin{Bmatrix} \dfrac{\partial}{\partial x} \\ \\ \dfrac{\partial}{\partial y} \\ \\ \dfrac{\partial}{\partial z} \end{Bmatrix}. \tag{5.57}$$

On multiplying by the inverse of the Jacobian matrix, we have the expression used for computing the derivatives of the shape functions defined on standard elements:

$$\begin{Bmatrix} \dfrac{\partial}{\partial x} \\ \\ \dfrac{\partial}{\partial y} \\ \\ \dfrac{\partial}{\partial z} \end{Bmatrix} = \begin{bmatrix} \dfrac{\partial x}{\partial \xi} & \dfrac{\partial y}{\partial \xi} & \dfrac{\partial z}{\partial \xi} \\ \\ \dfrac{\partial x}{\partial \eta} & \dfrac{\partial y}{\partial \eta} & \dfrac{\partial z}{\partial \eta} \\ \\ \dfrac{\partial x}{\partial \zeta} & \dfrac{\partial y}{\partial \zeta} & \dfrac{\partial z}{\partial \zeta} \end{bmatrix}^{-1} \begin{Bmatrix} \dfrac{\partial}{\partial \xi} \\ \\ \dfrac{\partial}{\partial \eta} \\ \\ \dfrac{\partial}{\partial \zeta} \end{Bmatrix}. \tag{5.58}$$

Computation of the first derivatives from a finite element solution in a given point is discussed in Section 7.1.

5.7 Stiffness matrices and load vectors

The algorithms for the computation of stiffness matrices and load vectors for three-dimensional elasticity are outlined in the following. Their counterparts for two-dimensional elasticity and heat conduction are analogous. The algorithms are based on eq. (4.21), however the integrals are evaluated element by element:

$$\int_{\Omega_k} ([D]\{v\})^T [E][D]\{u\}\, dV = \int_{\Omega_k} \{v\}^T \{F\}\, dV + \int_{\partial\Omega_k \cap \partial\Omega_T} \{v\}^T \{T\}\, dS + \int_{\Omega_k} ([D]\{v\})^T [E]\{\alpha\}\mathcal{T}_\Delta\, dV \tag{5.59}$$

where the differential operator matrix $[D]$ and the material stiffness matrix $[E]$ are as defined in Exercise 4.3.1. The kth element is denoted by Ω_k. The second term on the right hand side represents the virtual work of tractions acting on boundary segment $\partial\Omega_T$. This term is present only when one or more of the boundary surfaces of the element lies on $\partial\Omega_T$. For the sake of simplicity in presentation we assume that the number of degrees of freedom is the same for all three fields on Ω_k. We denote the number of degrees of freedom per field by n and define the $3 \times 3n$ matrix $[N]$ as follows:

$$[N] = \left[\begin{array}{cccc|cccc|cccc} N_1 & N_2 & \cdots & N_n & 0 & 0 & \cdots & 0 & 0 & 0 & \cdots & 0 \\ 0 & 0 & \cdots & 0 & N_1 & N_2 & \cdots & N_n & 0 & 0 & \cdots & 0 \\ 0 & 0 & \cdots & 0 & 0 & 0 & \cdots & 0 & N_1 & N_2 & \cdots & N_n \end{array}\right].$$

The jth column of $[N]$, denoted by $\{N_j\}$, is the jth shape function vector. We write the trial and test functions as linear combinations of the shape function vectors:

$$\{u\} = \sum_{j=1}^{3n} a_j \{N_j\} \quad \text{and} \quad \{v\} = \sum_{i=1}^{3n} b_i \{N_i\}. \tag{5.60}$$

5.7.1 Stiffness matrices

The elements of the stiffness matrix k_{ij} can be written in the form:

$$k_{ij}^{(k)} = \int_{\Omega_k} ([D]\{N_i\})^T [E][D]\{N_j\}\, dV. \tag{5.61}$$

We take advantage of the fact that two elements of $\{N_i\}$ are zero. The position of the zero elements depends on the value of the index i. For example when $1 \le i \le n$ then:

$$[D]\{N_i\} = \begin{Bmatrix} \partial/\partial x \\ 0 \\ 0 \\ \partial/\partial y \\ 0 \\ \partial/\partial z \end{Bmatrix} N_i = \underbrace{\begin{bmatrix} 1 & 0 & 0 \\ 0 & 0 & 0 \\ 0 & 0 & 0 \\ 0 & 1 & 0 \\ 0 & 0 & 0 \\ 0 & 0 & 1 \end{bmatrix}}_{[M_1]} \begin{Bmatrix} \partial/\partial x \\ \partial/\partial y \\ \partial/\partial z \end{Bmatrix} N_i = [M_1][J_k]^{-1} \begin{Bmatrix} \partial/\partial \xi \\ \partial/\partial \eta \\ \partial/\partial \zeta \end{Bmatrix} N_i$$

where $[J_k]^{-1}$ is the inverse of the Jacobian matrix corresponding to element k, see eq. (5.58), $[M_1]$ is a logical matrix. When the index i changes, only $[M_1]$ has to be replaced. Specifically, when $(n+1) \leq i \leq 2n$ then $[M_1]$ is replaced by $[M_2]$; when $(2n+1) \leq i \leq 3n$ then $[M_1]$ is replaced by $[M_3]$ which are defined as follows:

$$[M_2] := \begin{bmatrix} 0 & 0 & 0 \\ 0 & 1 & 0 \\ 0 & 0 & 0 \\ 1 & 0 & 0 \\ 0 & 0 & 1 \\ 0 & 0 & 0 \end{bmatrix} \qquad [M_3] := \begin{bmatrix} 0 & 0 & 0 \\ 0 & 0 & 0 \\ 0 & 0 & 1 \\ 0 & 0 & 0 \\ 0 & 1 & 0 \\ 1 & 0 & 0 \end{bmatrix}.$$

We define $\{\mathcal{D}\} := \{\partial/\partial\xi \ \partial/\partial\eta \ \partial/\partial\zeta\}^T$ and write eq. (5.61) in a form suitable for evaluation by numerical integration which is described in Appendix B:

$$k_{ij}^{(k)} = \int_{\Omega_{\text{st}}} \left([M_\alpha][J_k]^{-1}\{\mathcal{D}\}N_i\right)^T [E][M_\beta][J_k]^{-1}\{\mathcal{D}\}N_j |J_k| \, d\xi d\eta d\zeta. \tag{5.62}$$

The domain of integration is the appropriate standard element, i.e., hexahedral, tetrahedral of pentahedral element. The indices α and β take on the values 1, 2, 3 depending on range of the indices i and j. Therefore the element stiffness matrix $[K^{(k)}]$ consists of six blocks $[K_{\alpha\beta}^{(k)}]$:

$$[K^{(k)}] = \begin{bmatrix} [K_{11}^{(k)}] & [K_{12}^{(k)}] & [K_{13}^{(k)}] \\ & [K_{22}^{(k)}] & [K_{23}^{(k)}] \\ \text{sym.} & & [K_{33}^{(k)}] \end{bmatrix}. \tag{5.63}$$

Exercise 5.7.1 Refer to equations (3.66) to (3.70). Develop an expression for the computation of the terms of the stiffness matrix, analogous to $k_{ij}^{(k)}$ given by eq. (5.62), for axisymmetric elastostatic models.

5.7.2 Load vectors

The computation of element level load vectors corresponding volume forces, surface tractions and thermal loading is based on the corresponding terms on the right hand side of eq. (7.11).

Volume forces

Computation of the load vector corresponding to volume force $\{F\}$ acting on element k is a straightforward application of eq. (5.52):

$$r_i^{(k)} = \int_{\Omega_{\text{st}}} \{N_i\}^T \{F\} \, |J_k| \, d\xi d\eta d\zeta \qquad i = 1, 2, \ldots, 3n. \tag{5.64}$$

Surface tractions

Evaluation of the load vector terms corresponding to surface tractions depends on the side of the element on which the tractions are acting. For example, let us assume that traction vectors acting on a hexahedral element on the face $\zeta = 1$. In this case the ith term of the load vector is:

$$r_i^{(k)} = \int_{-1}^{+1}\int_{-1}^{+1} \{N_i\}^T \{T\} \left| \frac{\partial \vec{r}}{\partial \xi} \times \frac{\partial \vec{r}}{\partial \eta} \right|_{\zeta=1} d\xi d\eta$$

where the range of i is the set of indices of shape functions associated with the face $\zeta = 1$.

Thermal loading

The differential operator $[D]$ appears in the functional that represents thermal loading. Therefore the expression for $r_i^{(k)}$ depends on the index i.

$$r_i^{(k)} = \int_{\Omega_{\mathrm{st}}} \left([M_\beta][\mathcal{D}]\{N_i\}\right)^T [E]\{\alpha\}\mathcal{T}_\Delta \, |J_k| \, d\xi d\eta d\zeta \qquad i = 1, 2, \ldots, 3n$$

where $\beta = 1$ when $1 \leq i \leq n$, $\beta = 2$ when $(n+1) \leq i \leq 2n$ and $\beta = 3$ when $(2n+1) \leq i \leq 3n$. The matrices $[M_\beta]$ and the operator $\{\mathcal{D}\}$ are defined in Section 5.7.1.

5.8 Chapter summary

A finite element space is characterized by a finite element mesh and the polynomial degrees and mapping functions assigned to the elements of the mesh. The polynomial degrees identify a polynomial space defined on a standard element. The polynomial space is spanned by basis functions, called shape functions. Two kinds of shape functions, called Lagrange and hierarchic shape functions, were described for quadrilateral and triangular elements. The finite element space is spanned by the mapped shape functions subject to the requisite continuity requirements, discussed in Section 2.5.3.

Unless the mappings of all elements are polynomial functions of degree equal to or less than the polynomial degree of elements, rigid body rotation will not be represented exactly by the finite element solution. Nevertheless, rapid convergence to the correct solution will occur as the finite element space is progressively enlarged by h-, p-, or hp-extension. The mapping functions used in FEA must be such that the Jacobian determinant is positive in every point within the element.